Autonomous Latching System for Robotic Boats

Luis A. Mateos[12], Wei Wang[12], Banti Gheneti[12], Fabio Duarte[1], Carlo Ratti[1] and Daniela Rus[2]

***Abstract*— Autonomous robotic boats are devised to transport people and goods similar to self-driving cars. One of the attractive features specially applied in water environment is to dynamically link and join multiple boats into one unit in order to form floating infrastructure such as bridges, markets or concert stages, as well as autonomously self-detach to perform individual tasks.**

In this paper we present a novel latching system that enables robotic boats to create dynamic united floating infrastructure while overcoming water disturbances. The proposed latching mechanism is based on the spherical joint (ball and socket) that allows rotation and free movements in two planes at the same time. In this configuration, the latching system is capable to securely and efficiently assemble/disassemble floating structures. The vision-based robot controller guides the self-driving robotic boats to latch with high accuracy in the millimeter range. Moreover, in case the robotic boat fails to latch due to harsh weather, the autonomous latching system is capable to recompute and reposition to latch successfully. We present experimental results from latching and docking in indoor environments. Also, we present results in outdoor environments from latching a couple of robotic boats in open water with calm and turbulent currents.

I. Introduction

In robotics, there are two main methodologies for assembly structures with autonomous robots regardless of the environment (terrestrial / aerial / water). The first is robots transporting the building blocks for constructing the structure [1] [2]. The second method is robots attaching themselves to the structure as a building unit [3] [4].

In this study we follow the second methodology, in which the robot is a building unit. But first we introduce developments in autonomous underwater vehicles (AUV) docking stations and present how we embed these concepts in our autonomous latching system for robotic boats.

AUVs have extensive development of docking systems that protect and recharge the underwater robot [5] [6] [7] [8] [9] [10]. However, for robotic boats or autonomous surface vehicles (ASV), there are relatively limited research accomplishments, specifically in latching systems for docking to a station [11] [12] or to another boat or to multiple boats [13]. The main challenges are due to water and wind dynamics which cause disturbances such as movements, vibration and inclination on the boats.

*This work was supported by grant from the Amsterdam Institute for Advanced Metropolitan Solutions (AMS) in Netherlands.

[1]Massachusetts Institute of Technology, Senseable City Labs, 9-250 77 Massachusetts Avenue, Cambridge, MA 02139, US.

[2]Massachusetts Institute of Technology, Computer Science & Artificial Intelligence Laboratory, 32 Vassar St, Cambridge, MA 02139, US. {lamateos, wweiwang, bgheneti, fduarte, ratti, rus}@mit.edu

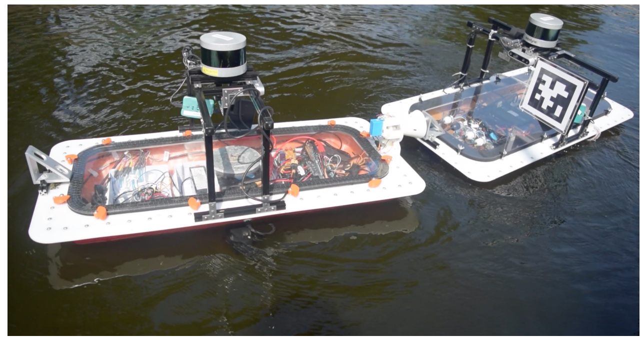

Fig. 1. Autonomous robotic boats latched in train link configuration.

A. Latching system for AUVs

The process to latch an AUV into a docking station is the following: The first step is *homing*. This step utilizes a tracking system to assist in guiding the AUV into the dock. This system is activated once the AUV is within a close range of distance to the docking station. In order to measure the distance between the AUV and a docking station, the following sensors can be applied: 1) Acoustic. This solution consists of an ultra short base line (USBL) with a range up to 30m with the accuracy of $\pm 0.2m$ [5] [6] [9] [14]. 2) Electromagnets. The electromagnetic solution is able to provide the orientation within a range up to 10m with the accuracy of $\pm 0.1m$ [7]. 3) Optics. The optical approach can be thermal [15] or visual [10] [16] with a range up to the visibility of the target (1m to 15m) and with high accuracy in the millimeter range.

The second step of latching is *docking*, which specifically refers to joining the AUV to a static docking station [17] [15] [16] [14]. Several docking components in AUVs have been widely considered by academy and industry. Among these are:

1) Framed modular garage. The tubular garage is commonly shaped as a cone or funnel, which helps minimize the level of precision required to dock the AUV by increasing the target size. In this way, the vehicle approaches the funnel entrance, while misalignments are mechanically corrected [15] [16] [14].

2) Stinger. This system is similar to the aircraft base stations, where the airplanes land with the help of a wired hook that latches on a predetermined slot [5].

Once docking is done, the next step is *garaging*, in which the vehicle is locked, securing its position. In this context, the locking mechanism can be as simple as a hook, or more elaborated system that involves active devices, such as motorized-screws [18].

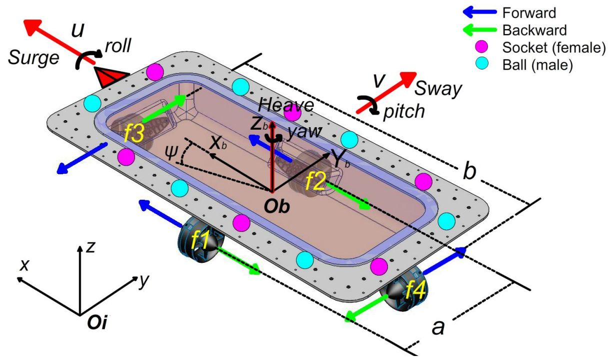

Fig. 2. Force vectors in the robotic boats.

B. Latching system for ASVs or robotic boats

The latching framework from O'Hara [13] is able to latch multiple boats with a hook-wire mechanism and overcome water disturbances. However, this latching system has several limitations: 1) The latching/unlatching requires the robotic boats to be spaced apart so the latching hook can rotate. This limitation restricts the possibility to dynamically detach one robot from a formed floating structure. 2) Also, the system relies on an overhead camera, instead of a distributed controller, as our self-driving robotic boats.

In this paper we present a novel latching system that enables autonomous robotic boats to dynamically create floating infrastructure in a secure and efficient way, while overcoming water disturbances, see Figure 1. The roboats, which are the robotic boats we placed the latching system on, are expected to navigate autonomously on the water canals of Amsterdam.

The proposed latching system takes into account the surge and sway vectors (motions) of the roboat, with a funnel to compensate the misalignment in the vertical axis (heave) from water disturbances or weight imbalances. Moreover, in certain configurations, the system only requires one actuator to perform the latching of two boats.

This paper is structured as follows: Section II introduces the design of our robotic boats, thrusters configuration, mechanical model of the latching system and its functional modes. Section III describes the model and controller our robotic boats use to navigate. Section IV describes the guiding controller for latching. Section V presents the algorithm and control strategy for latching. Section VI shows the results from the indoor swimming pool and outdoor test on the Charles River in Boston, US. Conclusions are proposed in Section VII, which also point out some of the next steps and future challenges.

II. Design

The aim of the autonomous latching system is to enable robotic boats to latch to a docking station and to other roboats for creating floating infrastructure, such as bridges, floating markets and stage concerts. Therefore, the system is required to latch fast, secure and efficiently, while overcoming water disturbances and misalignments.

A. Robotic boat

The robotic boat consists of a rectangular base (2:1 ratio) with four thrusters in the middle of its edges, see Figure 2. In this relationship the roboat is able to move forward, backward, sideways and is able to rotate on its axis. The dimensions of this robotic platform are $1000mm \times 500mm \times 150mm$.

The perception and localization of the roboat are performed by a VLP16 lidar (16 lines) located at the top of the boat. Also, the robotic boats integrate a skirt of Intel Realsense cameras to detect tags in the docks and on other roboats for position estimation and identification. The system integrates an IMU for recognition of inclination and velocities.

B. Latching mechanism

The latching system is based on the $ball-socket$ joint, which allows a rotation about each of the three rectangular axes. Each robotic boat integrates the two components of the spherical joint and the number of connectors can be tailored for each use case; i.e., in the towing use case, robotic boats with connectors on the front and back can latch in train link configuration and to a docking station. Moreover, if the conectors are added on the sides of the roboats, the boats can create a floating platform. In this way, the spherical joint created between the connected roboats enables them to rotate and move on the surge and sway vectors while overcoming wave disturbances.

The latching system considers two cases: when a roboat is latching to a docking station and when a roboat is connecting to another roboat.

It is important to define these cases, because when latching to a dock, we don't want that the components on the dock to require power. We expect passive elements that do not require maintenance, nor connections for power in any means. On the other hand, when putting together two roboats, both components can be powered for integrating sensors and actuators in order to help with the latching of the two floating robotics platforms.

In this framework, there are three connecting components:

1) Passive Ball (male): The passive male part is used only on docks, it consists of a central axis covered with a 3D printed protective rubber as a damping element and a ball on the front-edge, see Figure 3*a*. The pins also integrate a floating device to maintain their positions with respect to the water level to be in the same level as the floating robotic boats.

2) Active Ball (male): The active male part is integrated on the roboats and can be extended or contracted with a linear actuator when reaching for the connection on other roboats. This actuation is required for adding roboats into an already formed floating platform.

3) Socket (female): The female part consists of a funnel to guide the male ball into an actuated receptor that traps the ball, creating the spherical joint between the parts, see Figure 3*b*. The receptor consists of three arms that are guided

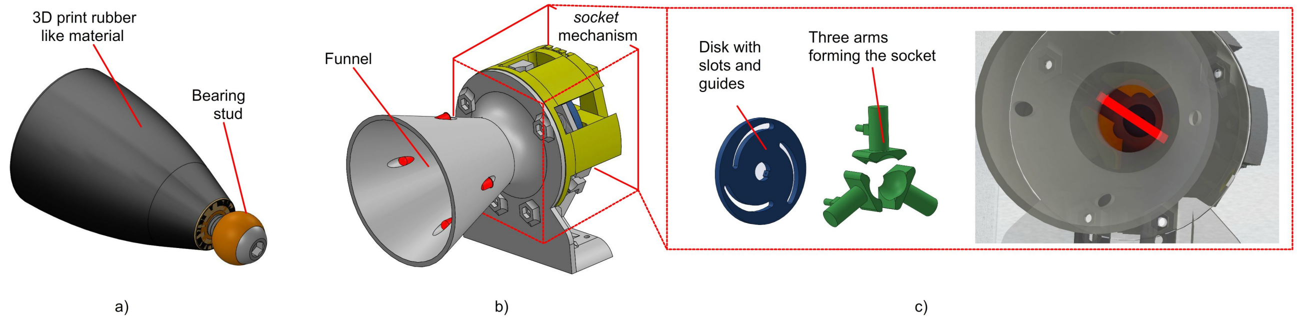

Fig. 3. a) Passive male integrates a bearing stud on the front of the pin and 3D printed soft plastic as damping element. b) Socket (female) integrates a funnel to guide the male ball into a receptor that traps the ball. This receptor integrates a mechanism with three arms that when closed forms the ball-socket. Also, integrates a laser system to detect when the pin is inside to close the socket. c) Socket elements: disk with guides, three arms, one servomotor and the ball detection system with laser crossing the socket.

by a disk, enabling the actuation of the arms with only one servomotor.

The ball's socket is created when the arms are closed and when opened the arms released the trapped bearing stud. This receptor integrates an electric system similar to the security systems, in which a laser beam activates an alarm. In our case, the laser beam is crossing the open socket to detect if the ball is inside the socket space. So when the laser is blocked by the ball, it reacts by rotating the disk, closing the socket and trapping the ball, creating the spherical joint, see Figure 3*c*.

C. Passive markers

The roboats are required to dock in the Amsterdam canals, which are a historical heritage site. Thus, our methodology should be minimally invasive to the canal walls and should not integrate any active tags that require a power supply (i.e. lamp or infrared). For this reason, we propose the apriltags method for guiding the roboats to docking stations. These tags offer a good framework for detection and identification, plus can be customized [19]. Moreover, the apriltags on the dock side can be made of tiles or stones to be less invasive.

III. Model

The dynamics and model of our robotic boats were defined in [20]. The robotic boats implement model predictive control (MPC) for navigation. The applied force and moment vector $\boldsymbol{\tau}$ is:

$$\boldsymbol{\tau} = \mathbf{B}\mathbf{u} = \begin{bmatrix} 1 & 1 & 0 & 0 \\ 0 & 0 & 1 & 1 \\ \frac{a}{2} & -\frac{a}{2} & \frac{b}{2} & -\frac{b}{2} \end{bmatrix} \begin{pmatrix} f_1 \\ f_2 \\ f_3 \\ f_4 \end{pmatrix} \qquad (1)$$

where $\mathbf{B}$ is the control matrix describing the thruster configuration and $\mathbf{u}$ is the control vector. a is the distance between the transverse propellers and b is the distance between the longitudinal propellers, f_1, f_2, f_3 and f_4 are the forces generated by the corresponding propeller, see Figure 2. Each propeller is fixed and can generate continuous forward and backward forces.

IV. Guiding Controller

The roboats are configured in swarm fashion, meaning that each robot is an independent entity and that there is no direct communication between them, only by visual cues.

The main reason for integrating apriltags in our autonomous latching system is that the roboat's localization based on lidar with NDT matching has an accuracy in the range of $\pm 100mm$. However, this precision is not enough for putting together the boats on open water, since an accuracy in the range of $\pm 40mm$ is required to perform the latching.

In this context, the robotic boats implement the "low" accuracy localization $\pm 100mm$ when performing path planning and obstacle avoidance, while the "high" accuracy of $\pm 40mm$ is implemented in short distances. Specifically, when the camera is able to find the apriltag and the boats are a couple of meters apart from each other and within $\pm 27.5°$.

The latching system assumes that the roboats and the docking station are floating at similar levels above the water, so the misalignment from waves is compensated by the funnel, see Figure 4.

A. Working space - simplifying 3D space into a 2D plane

The controllable space is defined by a 2D x - y plane on the water. This is to simplify the problem from 3D space to a 2D plane. Since, we don't take into account the *heave* vector, as this is compensated by the funnel and in our assumption all elements are floating on the water, see Figure 5.

The distances and angles between two roboats are given by three variables:

- dx is the difference in position in the x-axis (the distance between the entities)
- dy is the difference in position in the y-axis (the distance to the left or to the right)
- ψ is the angle between the two entities

B. Guiding controller

In this section, we present our methodology to latch a couple of roboats, R_2 and R_3, resulting in a new floating platform $R_{23} = R_2 \cup R_3$. We use the trajectory controller with the passive marker detection to guide the robotic boat to latch to another roboat on the open water.

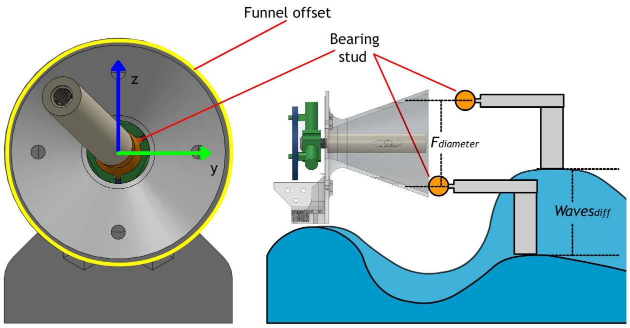

Fig. 4. The funnel compensates water level differences from the waves in the $z-axis$, and also misalignments in the $y-axis$ from the guiding controller.

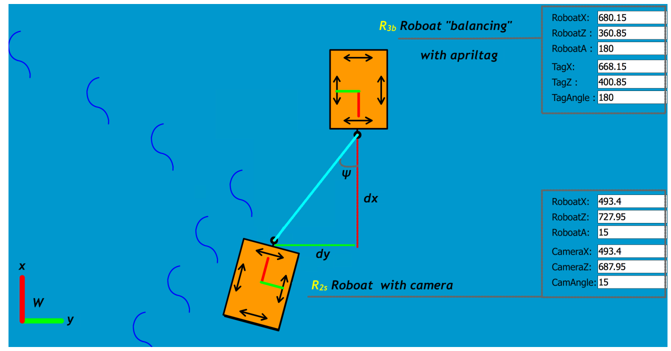

Fig. 5. 2D simulation environment for latching roboats, $R2_{dy}$ is the lateral distance between parts, $R2_{dx}$ is the distance between them and angle $R2_{\psi}$.

In our approach, one robotic platform waits in a position, similar to a "balancing" robot, becoming a pseudo-docking station, while the other roboat performs the movements for latching.

1) Balancing robot : In the balancing robot state, we want the robotic boat to maintain a certain position x^*.

2) Latching action : In order to latch the robotic platforms R_2 to R_3, we take as reference a pair of connectors (s,b), socket (female) and ball (male), such that $s \in R_2$ and $b \in R_3$. In this configuration, module s latches to b, and it docks through the x axis of R_3. The position of the connector s in the coordinate frame of connector b, R_3, is denoted by $(x_s^{(b)}, y_s^{(b)}, z_s^{(b)})$.

The docking method can be modeled as an intensity function $\bigtriangledown f$, which is followed by the guiding controller as:

$$w_R = \bigtriangledown f(x_s^{(b)}, y_s^{(b)}, z_s^{(b)}) \tag{2}$$

The intensity function is defined as the acceptance ratio by the conical funnel, which is a cone with radius $r = 40mm$, height $h = 80mm$ and aligned with the roboat R_3 $x-axis$. In this case, the radius r defines the maximum error that is tolerable during docking, e.g. misalignment error ($error < \pm 40mm$) that is adjusted by the mechanical funnel.

The funnel acceptance angle is 27.5°, meaning that if the ball b is moving with a constant velocity v, it will move towards the socket s. Otherwise, the latching may fail and the roboat must retake its initial position for the guiding controller to reposition itself and retry the latching algorithm.

V. Latching Controller

In order to read the actual angle between the camera and the apriltag, the tag detection requires that the camera and the tag are with the same orientation. At the same time, to estimate the actual orientation between them, the tag detection requires that the camera is directly facing the tag. Therefore, the latching controller integrates a hybrid control strategy which tries to position the camera to face the tag with the same orientation.

The latching controller integrates three PD controllers:

- Control I: Minimize lateral distance $dy_{s,b} = R3_{dy} - R2_{dy}$
- Control II: Minimize longitudinal distance $dx_{s,b} = R3_{dx} - R2_{dx}$
- Control III: Minimize the angle ψ between the entities

The hybrid controller initially tries to set the roboats to have the same orientation by minimizing $dy_{s,b}$ and the angle ψ between them. If the error is greater than the tolerances, the latching roboat R_2 is set to maintain a distance of $1000mm$ from the target to keep minimizing these errors until the error from Control I and Control III are inside the funnel tolerances. Then R_2 (roboat with the socket) moves forward minimizing $dx_{s,b}$, while combining the lateral distance and angle strategies to latch the balancing roboat R_3 with the ball, see Algorithm 1.

Algorithm 1 Latching algorithm

Require: $dy_{s,b}, dx_{s,b}, \psi, flag\_missed\_target$
Ensure: Camera targeting tag
  min($dy_{s,b}$)
  min(ψ)
  if $flag\_missed\_target == 0$ **then**
    if $dx_{s,b} > 0mm$ **then**
      if $dy_{s,b} < 10mm$ **or** $\psi < 2°$ **then**
        min($dx_{s,b}$)
      else
        Move back $1m$ and keep minimizing $dy_{s,b}$ and ψ
        min($dx_{s,b}$ - $1m$)
      end if
    else
      $flag\_missed\_target = 1$
    end if
  end if
  if $flag\_missed\_target == 1$ **then**
    Go to initial position and retry to latch
    min($dx_{s,b}$ - $1m$)
    if $dx_{s,b} > 1m$ **then**
      flag_missed_target = 0
    end if
  end if

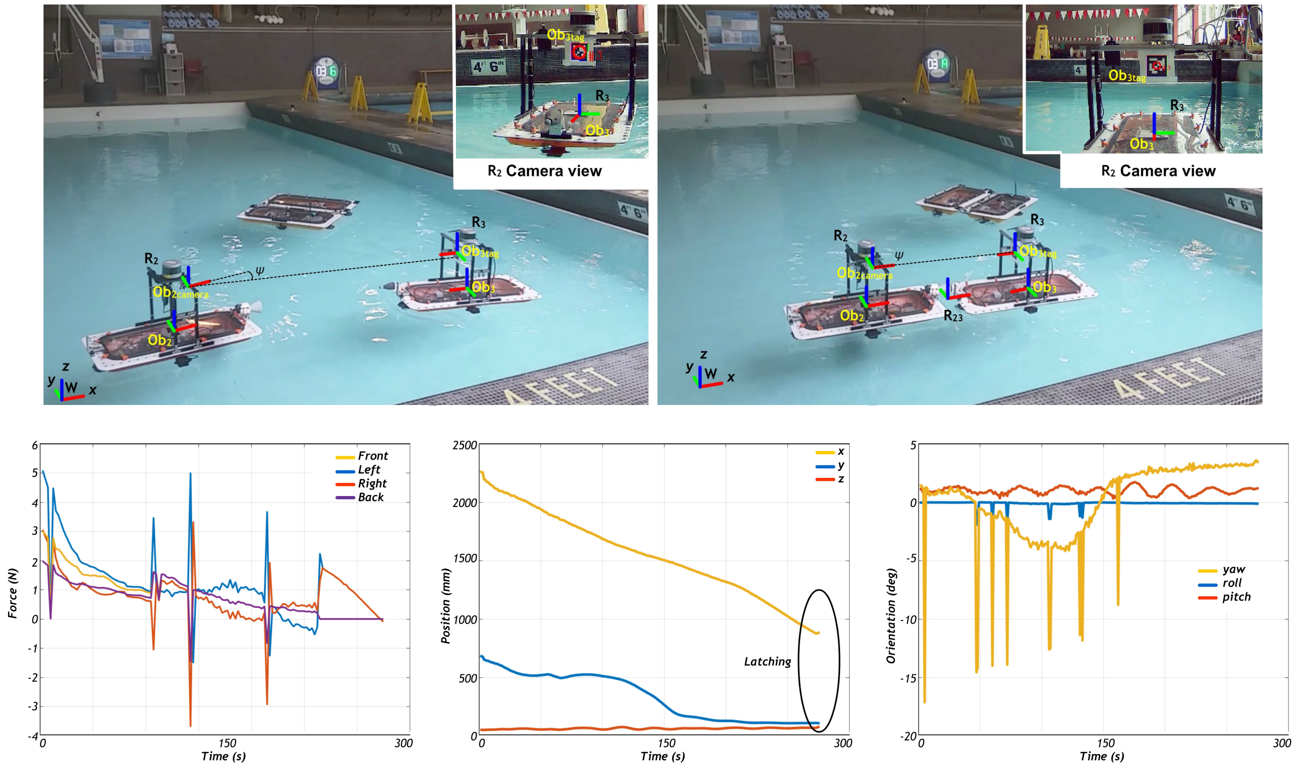

Fig. 6. Indoor experiment. Roboats coordinate frames R_2, R_3 and new formed robotic platform R_{23} (top). Roboats performing latching, R_2 forces (bottom-left), R_2 position (bottom-center), R_2 orientation (bottom-right).

VI. Experiments

This section contains the results from our developed latching system tested indoors and outdoors. The experimental results validate the mechanical design and the guiding controller used for accurately positioning the roboats side to side for latching.

A. Indoor experiments at MIT - swimming pool

Tests were performed in a swimming pool, with dimensions of $20m \times 10m \times 1.5m$. In this facility the water is calm with minimal disturbances (roboat *roll*, *pitch* and *yaw* angles $RPY \leq 1°$).

1) Latching to a "balancing" roboat : The roboat with the ball R_3 autonomously keeps its position "balancing" waiting to be latched by the roboat with the socket R_2. In this setup, the roboat R_2 navigates from one corner of the swimming pool to face the "balancing" roboat and then activates the guiding controller to perform latching, see Figure 6.

The roboat that is balancing is not completely static. It is oscillating its position d_x and d_y $\pm 50mm$ and orientation $RPY \pm 1°$, creating a challenging situation for the guiding algorithm, since it's required to adapt its position and orientation to a moving target.

Figure 6 shows the forces, position and orientation for a successful latching between the roboats. In this case, the position in d_x must be $< 900mm$ since the camera and target are mounted in the center of the roboats, the position in $d_y < \pm 40mm$ and the angle $yaw < \pm 27.5°$. Even though the orientation registered noisy peaks, the plot from the position of the roboat shows a smooth drive, minimizing the distance to the target d_x, from $2250mm$ to $900mm$, and minimizing the lateral distance d_y, from $70mm$ to $< 10mm$.

B. MIT Sailing pavilion - Charles River (outdoor)

In this location, we tested the most challenging latching, which is between two roboats. We tested and registered data a couple of times in different dates. In one test we registered *pitch* and *roll* angles up to $\pm 1.5°$, similar to the registered angles in the roboat's working environment (Amsterdam canals). We will refer to this test as the "calm" water test. In addition, another test was performed in "turbulent" water with registered *pitch* and *roll* angles up to $\pm 5°$.

In both experiments the roboats where able to latch. However the roboat misses the target the first time, then recomputes the position and orientation of the target to autonomously retry and latch successfully the following times.

In the calm water experiment, the balancing roboat registered an error in position in the range of $\pm 100mm$ and an error in orientation: *roll* $\pm 1°$, *pitch* $\pm 1.5°$ and a *yaw* $\pm 2°$. While in the turbulent water experiment, the error in position was $\pm 200mm$, and, the error in orientation: *roll* $\pm 1°$, *pitch* $\pm 5°$ and a *yaw* $\pm 2°$, see Table I. The causes of missing the target were: the error in position and orientation of the balancing roboat and the reflections of light on the framed apriltag perceived by the camera.

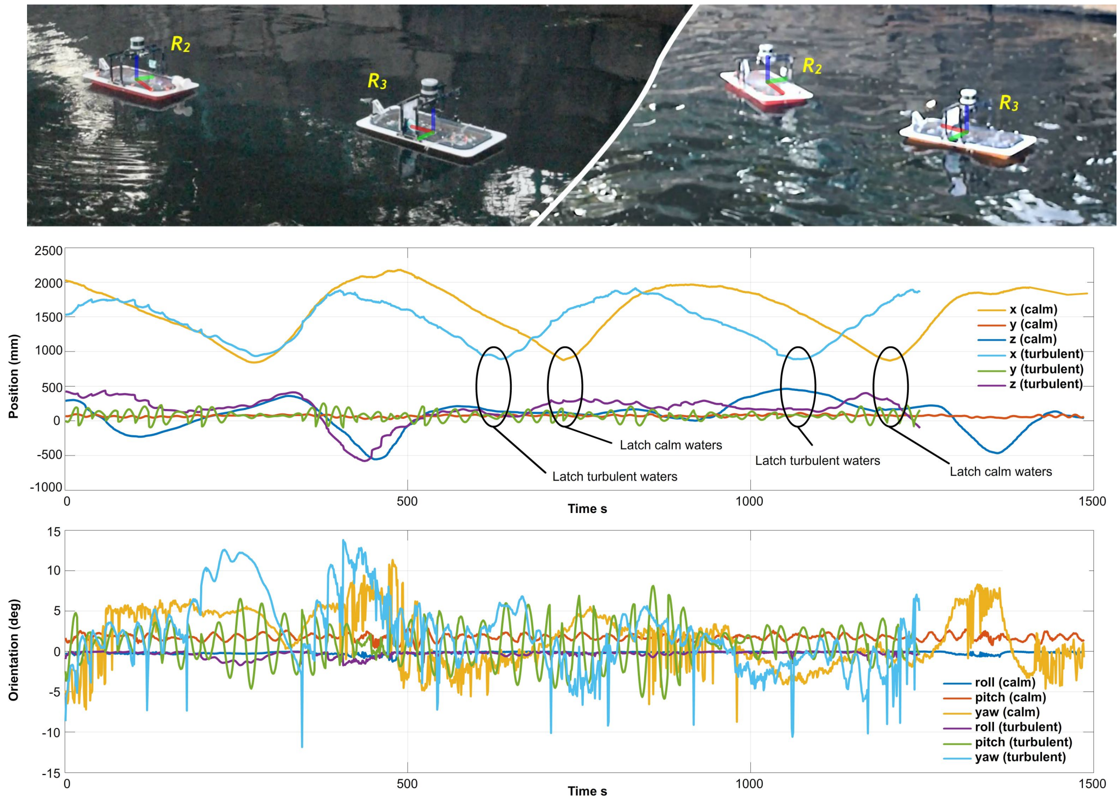

Fig. 7. Experimental results from roboats performing latching in open water (same test, different days, same location at Charles River, Boston). Roboats in calm water and roboats in turbulent water (top). The roboats in calm water registered pitch and roll angles in the range $\pm 1.5°$ and were able to latch a couple of times after one missed attempt. In the same way, the roboats in turbulent water registered pitch and roll angles in the range $\pm 5°$ and were able to latch a couple of times after one missed attempt.

TABLE I

BALANCING ROBOAT ERROR AND LATCHING SUCCESS RATE (20 ATTEMPTS PER EXPERIMENT).

	Balancing error position (mm) and angle ($°$)	**First attempt effectivity successful rate**
Indoors	*dx, dy and angle*	*percentage*
Latching to a dock	0	99%
Latching to a docked roboat	$d_x, d_y \approx 20mm$ $RPY \approx 1°$	95%
Latching to a balancing roboat	$d_x, d_y \approx 50mm$ $RPY \approx 1°$	80%
Outdoors	*dx, dy and angle*	*percentage*
Latching to a balancing roboat in calm water	$d_x, d_y \approx 100mm$ $R \approx 1°$, $P \approx 1.5°$ $Y \approx 2°$	50%
Latching to a balancing roboat in turbulent water	$d_x, d_y \approx 200mm$ $R \approx 1°$, $P \approx 5°$ $Y \approx 2°$	33%

Figure 7 shows the experimental results from the calm and turbulent water tests. The roboat R_2 with socket wants to latch to the balancing R_3. The plots reveal the position and orientation for a one miss and two latch sequence in both experiments. In the plot it is easy to notice how the *pitch* angle from the roboat was affected by the waves. Also, it is possible to notice the water current in the plots. The roboat R_2 reaches the latching point faster in the turbulent test. In these experiments, the roboats are latched when the position $d_x < 900mm$, $d_y < \pm 40mm$ and $yaw < \pm 27.5°$.

VII. CONCLUSION AND FUTURE WORK

This paper presents an autonomous latching system for self-driving robotic boats. The system is able to latch efficiently to a docking station and to another robotic boat while overcoming water disturbances and misalignments. The system is mechanically reliable, based on the spherical joint principle that enables rotation and movement in two directions between the latched parts.

In our framework, the roboats work in swarm fashion, which means that each robot is an independent entity and there is no direct communication between them. The roboats are guided globally by the path planning and obstacle avoidance algorithms with positioning errors in the range of $\pm 100mm$. However, the positioning errors must be $< 40mm$ for performing latching between roboats on open water. Therefore, we developed a vision based guiding controller able to position the roboats with high accuracy for latching.

The experiments were performed in an indoor swimming pool and outdoors, on the Charles River in Boston, US. In the experiments, the autonomous latching system showed good results when latching a couple of roboats in extreme turbulent environments with waves that tilt the roboats $\pm 5°$ in *pitch* and *roll*. In this difficult environment, the guiding system misses the target in its first attempt. However, it autonomously adapts by repositioning the roboat to retry and successfully latches to the floating roboat.

References

[1] J. Werfel and R. Nagpal, "Three-dimensional construction with mobile robots and modular blocks," *The International Journal of Robotics Research*, vol. 27, no. 3-4, pp. 463–479, 2008. [Online]. Available: https://doi.org/10.1177/0278364907084984

[2] F. Augugliaro, S. Lupashin, M. Hamer, C. Male, M. Hehn, M. W. Mueller, J. S. Willmann, F. Gramazio, M. Kohler, and R. D'Andrea, "The flight assembled architecture installation: Cooperative construction with flying machines," *IEEE Control Systems*, vol. 34, no. 4, pp. 46–64, Aug 2014.

[3] S. Murata, H. Kurokawa, and S. Kokaji, "Self-assembling machine," in *Proceedings of the 1994 IEEE International Conference on Robotics and Automation*, May 1994, pp. 441–448 vol.1.

[4] B. T. Kirby, B. Aksak, J. D. Campbell, J. F. Hoburg, T. C. Mowry, P. Pillai, and S. C. Goldstein, "A modular robotic system using magnetic force effectors," in *2007 IEEE/RSJ International Conference on Intelligent Robots and Systems*, Oct 2007, pp. 2787–2793.

[5] G. Griffiths, N. Millard, and R. Rogers, *Logistics, Risks and Procedures concerning Autonomous Underwater Vehicles*. CRC Press, 2017/08/09 2002, pp. 279–293. [Online]. Available: https://doi.org/10.1201/9780203522301.ch16

[6] "Underwater mobile docking of autonomous underwater vehicles," in *2012 Oceans*, Oct 2012, pp. 1–15.

[7] M. D. Feezor, P. R. Blankinship, J. G. Bellingham, and F. Y. Sorrell, "Autonomous underwater vehicle homing/docking via electromagnetic guidance," in *OCEANS '97. MTS/IEEE Conference Proceedings*, vol. 2, Oct 1997, pp. 1137–1142 vol.2.

[8] B. Allen, T. Austin, N. Forrester, R. Goldsborough, A. Kukulya, G. Packard, M. Purcell, and R. Stokey, "Autonomous docking demonstrations with enhanced remus technology," in *OCEANS 2006*, Sept 2006, pp. 1–6.

[9] B. W. Hobson, R. S. McEwen, J. Erickson, T. Hoover, L. McBride, F. Shane, and J. G. Bellingham, "The development and ocean testing of an auv docking station for a 21" auv," in *OCEANS 2007*, Sept 2007, pp. 1–6.

[10] A. Martins, J. M. Almeida, H. Ferreira, H. Silva, N. Dias, A. Dias, C. Almeida, and E. P. Silva, "Autonomous surface vehicle docking manoeuvre with visual information," in *Proceedings 2007 IEEE International Conference on Robotics and Automation*, April 2007, pp. 4994–4999.

[11] A. R. Girard, J. B. de Sousa, and J. K. Hedrick, "Dynamic positioning concepts and strategies for the mobile offshore base," in *ITSC 2001. 2001 IEEE Intelligent Transportation Systems. Proceedings (Cat. No.01TH8585)*, 2001, pp. 1095–1101.

[12] G. Remmers, R. Zueck, P. Palo, and R. Taylor, "Mobile offshore base," 2017.

[13] I. O'Hara, J. Paulos, J. Davey, N. Eckenstein, N. Doshi, T. Tosun, J. Greco, J. Seo, M. Turpin, V. Kumar, and M. Yim, "Self-assembly of a swarm of autonomous boats into floating structures," in *2014 IEEE International Conference on Robotics and Automation (ICRA)*, May 2014, pp. 1234–1240.

[14] K. Teo, B. Goh, and O. K. Chai, "Fuzzy docking guidance using augmented navigation system on an auv," *IEEE Journal of Oceanic Engineering*, vol. 40, no. 2, pp. 349–361, April 2015.

[15] J. Y. Park, B. H. Jun, P. M. Lee, F. Y. Lee, and J. h. Oh, "Experiment on underwater docking of an autonomous underwater vehicle 'isimi' using optical terminal guidance," in *OCEANS 2007 - Europe*, June 2007, pp. 1–6.

[16] P.-M. Lee, B.-H. Jeon, and S.-M. Kim, "Visual servoing for underwater docking of an autonomous underwater vehicle with one camera," in *Oceans 2003. Celebrating the Past ... Teaming Toward the Future (IEEE Cat. No.03CH37492)*, vol. 2, Sept 2003, pp. 677–682 Vol.2.

[17] P. Jantapremjit and P. A. Wilson, "Optimal control and guidance for homing and docking tasks using an autonomous underwater vehicle," in *2007 International Conference on Mechatronics and Automation*, Aug 2007, pp. 243–248.

[18] L. Mateos and M. Vincze, "Lammos - latching mechanism based on motorized-screw for reconfigurable robots," in *Advanced Robotics (ICAR), 2013 16th International Conference on*, Nov 2013, pp. 1–8.

[19] E. Olson, "Apriltag: A robust and flexible visual fiducial system," in *2011 IEEE International Conference on Robotics and Automation*, May 2011, pp. 3400–3407.

[20] W. Wang, L. A. Mateos, S. Park, P. Leoni, B. Gheneti, F. Duarte, C. Ratti, and D. Rus, "Design. modeling, and nonlinear model predictive tracking control of a novel autonomous surface vehicle," in *2018 IEEE International Conference on Robotics and Automation (ICRA)*, May 2018, pp. 1–5.